

# Network Harness: Metropolis Public Transport

C. von Ferber,<sup>1,2,\*</sup> T. Holovatch,<sup>3</sup> Yu. Holovatch,<sup>4,5,3</sup> and V. Palchykov<sup>3</sup>

<sup>1</sup>*Complex Systems Research Center, Jagiellonian University, 31007 Kraków, Poland*

<sup>2</sup>*Physikalisches Institut, Universität Freiburg, 79104 Freiburg, Germany*

<sup>3</sup>*Ivan Franko National University of Lviv, 79005 Lviv, Ukraine*

<sup>4</sup>*Institute for Condensed Matter Physics of the National Academy of Sciences of Ukraine, 79011 Lviv, Ukraine*

<sup>5</sup>*Institut für Theoretische Physik, Johannes Kepler Universität Linz, 4040 Linz, Austria*

We analyze the public transport networks (PTNs) of a number of major cities of the world. While the primary network topology is defined by a set of routes each servicing an ordered series of given stations, a number of different neighborhood relations may be defined both for the routes and the stations. The networks defined in this way display distinguishing properties, the most striking being that often several routes proceed in parallel for a sequence of stations. Other networks with real-world links like cables or neurons embedded in two or three dimensions often show the same feature - we use the car engineering term *harness* for such networks. Geographical data for the routes reveal surprising self-avoiding walk (SAW) properties. We propose and simulate an evolutionary model of PTNs based on effectively interacting SAWs that reproduces the key features.

PACS numbers: 89.75.Hc, 89.75.Da, 89.40.Bb

## INTRODUCTION

Taken the general interest in networks of man-made and natural systems [1], it is remarkable that one of the most commonly encountered networks, the urban public transport network (PTN), is much less studied. The PTN constitutes an example of a transportation network and shares general features of these systems: evolutionary growth, optimization, embedding into two-dimensional (2D) space. However, as compared with other transportation networks like airport networks [2, 3], railway networks [4], or power grid networks [2, 5] much less is known about the statistical and topological properties of PTNs.

The few studies that have considered these questions so far have either been performed on a subnetwork (tram, subway) of a specific city like Boston or Vienna [6, 7, 8] or they were limited by the number of cities or their size. The recent thorough study of the bus and tram networks of 22 Polish cities considered PTNs with up to 2811 stations [9]. Our preliminary work on some larger networks [10] was restricted to only three cities (Berlin, Düsseldorf, and Paris). The present picture that emerges from this research views PTNs as networks with small-world properties and hierarchical organization as derived from various network characteristics and their correlations [9]. While indications for scale-free behavior have been found these depend strongly on the interpretation of the network.

The present article is based on a survey of selected major cities of the world with PTN sizes ranging between 2000 and 46000 stations. Simulations of an evolutionary growth model based on self-avoiding walks that we propose appear to reproduce most of the key features of these PTNs. In addition to the standard characteristics of complex networks like the number of nearest neighbors, mean

path length, and clustering we observe features specific to PTNs due to their embedding in geographic space constrained by city structure. The most striking being that often several routes proceed in parallel on a common road or track for a sequence of stations. While other networks with real-world links like cables or neurons embedded in two or three dimensions often show similar behavior, these can be studied in detail in our present case.

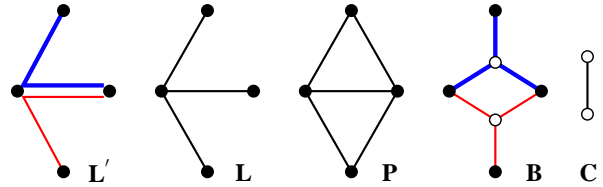


FIG. 1: PTN graph representations.  $L'$ -space: filled circles represent stations serviced by two different routes shown by a bold and a thin line.  $L$ -space: reduction of  $L'$  to a simple graph with single links.  $P$ -space: any two stations that are serviced by a common route are linked.  $B$ -space: stations are linked to the routes (open circles) they belong to.  $C$ -space: routes are connected when they share a common station.

From maps of PTNs it is obvious that routes in general do not follow the shortest path between their terminal stations but rather meander through neighborhoods and between sites of interest. We quantify this behavior by analyzing geographical data. This leads us to model the routes as self-avoiding walks that efficiently cover the surface while the sites of interest introduce an effective attraction between them.

To work out the specific features of PTNs, it is natural to interpret the public transport system of a city in terms of graphs, see Fig. 1. The primary network representation, which we call  $L'$ -space is defined by a set of routes each servicing an ordered series of stations. For

the PTNs studied so far, two different neighborhood relations were used that lead to different representations. In the first one, called **L**-space, two stations are defined as neighbors only if one station is the successor of the other one in the series of stations serviced by a route [7]. In the second one, the **P**-space, two stations are neighbors whenever they are serviced by a common route [4]. Some of the specific features found in PTNs are more naturally described in additional representations that we introduce. A bipartite graph, **B**-space, is constructed by

representing both routes and stations as nodes of different type as depicted by filled and open circles in Fig. 1. The one-mode projection of the **B**-space graph to the station nodes leads back to the **P**-space representation, whereas the corresponding projection to the set of routes results in a complementary **C**-space graph. Note that **L'** differs from **L** only by the presence of multiple links. In a similar fashion one may define additional primed spaces **P'**, **C'** by keeping multiple links also in **P** and **C** [11].

City	$N$	$M$	$\kappa$	$\kappa_p$	$\gamma$	$\hat{k}$	$\hat{k}/\bar{k}$	$\gamma_p$	$\hat{k}_p$	$\hat{k}_p/\bar{k}_p$	$\bar{C}$	$C$	$\bar{C}_p$	$C_p$	$\bar{\ell}$	$\bar{\ell}_p$	$\hat{\ell}_p$	$\bar{\ell}_p$
Berlin	2997	218	3.16	80.2	(4.30)	1.24	0.49	(5.86)	38.5	0.70	0.08	91.58	0.81	43.22	88	21.60	6	3.10
Dallas	7163	131	2.22	136.3	4.99	(1.01)	0.49	(4.67)	76.9	0.77	0.01	37.87	0.97	63.34	269	85.80	10	3.78
Düsseldorf	1615	124	3.20	90.3	(3.99)	1.12	0.44	(4.63)	58.8	1.02	0.04	22.91	0.79	20.99	56	13.18	5	2.58
Hamburg	8159	708	3.25	78.4	(4.70)	1.47	0.56	(4.92)	55.6	1.11	0.08	255.59	0.82	133.99	158	39.71	11	4.78
Hong Kong	2117	321	5.22	230.1	(3.04)	2.60	0.72	(4.40)	125.0	1.01	0.16	92.33	0.73	12.51	60	11.11	4	2.26
Istanbul	4043	414	2.69	140.1	4.04	(1.13)	0.49	(2.70)	71.4	0.93	0.03	44.99	0.79	41.54	131	29.69	6	3.09
London	11026	2005	3.23	213.9	4.58	(1.46)	0.48	4.39	(142.9)	1.27	0.16	658.15	0.70	78.51	77	22.03	6	3.19
Los Angeles	46244	1893	2.73	154.4	4.88	(1.50)	0.64	3.92	(200.0)	2.07	0.03	599.68	0.90	430.68	247	43.55	14	4.60
Moscow	3756	679	7.94	129.7	(3.31)	2.12	0.65	(2.91)	50.0	0.78	0.11	129.78	0.74	43.14	28	7.07	5	2.52
Paris	4048	232	6.41	79.5	2.61	(3.24)	0.94	3.70	(100.0)	2.07	0.07	86.78	0.88	72.88	47	7.22	5	2.79
Rome	6315	681	3.02	86.4	4.39	(1.16)	0.45	(5.87)	45.5	0.76	0.03	69.19	0.73	76.93	93	29.64	8	3.58
São Paulo	7223	998	5.95	333.6	2.72	(4.20)	1.29	(3.06)	200.0	1.46	0.23	514.11	0.73	38.32	33	10.34	5	2.66
Sydney	2034	596	4.35	73.2	3.99	(1.82)	0.55	(5.66)	38.5	0.91	0.14	87.66	0.73	34.92	35	12.71	7	3.03
Taipei	5311	389	4.02	415.5	(3.74)	1.75	0.56	(5.17)	200.0	0.85	0.11	188.89	0.69	15.38	74	20.86	6	2.35
$a=0, b=0.1$	635	500	2.77	216.6	–	–	–	4.43	(76.9)	0.47	–	–	0.76	2.9	110	36.10	4	1.96
$a=0, b=0.5$	3336	500	3.14	302.7	–	–	–	(7.66)	111.1	0.62	–	–	0.68	12.6	190	49.21	7	3.00
$a=0, b=8$	5464	500	3.36	233.8	–	–	–	(12.35)	71.4	0.46	–	–	0.65	22.8	229	59.37	9	3.71

TABLE I: PTN characteristics in **L**- and **P**-representations. Index 'p' indicates **P**-space characteristics. The last three rows show data for simulated cities. We list the number of stations  $N$ , the number of routes  $M$ , the ratio  $\kappa$  of the second  $k^2$  to the first moment  $\bar{k}$  of  $p(k)$ , the exponent  $\gamma$ , and the scale  $\hat{k}$  of fits of  $p(k)$  to power and exponential laws and the ratio  $\hat{k}/\bar{k}$ , the average clustering coefficient  $\bar{C}$  and its ratio  $C$  to the ER-value  $C_{ER} = \bar{k}/N$ , the maximal  $\bar{\ell}$  and the mean  $\bar{\ell}_p$  shortest path lengths; e.g.. an average trip between the 11026 London stations needs  $\bar{\ell}_p=3.2$  changes with a maximum of  $\hat{\ell}_p=6$ ; see text.

For our empirical survey we acquired publicly available data of the PTNs of 14 major cities from the web-pages of local public transport organizations [12]. Table I lists cities together with some of the characteristics extracted from our analysis. A more complete account will be given in a separate publication [11]. To check for the small-world properties of the networks we have analyzed the mean and maximal shortest path lengths  $\bar{\ell}$ ,  $\hat{\ell}$ . The data for space **L** given in Table I show that these numbers are very small as compared to the number of nodes. In the **P**-space the shortest path lengths  $\bar{\ell}_p$ ,  $\hat{\ell}_p$  correspond to the number of changes one should make traveling between two given stations. From these data we conclude that a typical station is within relatively short reach from all other stations. As has been shown [13],

small world networks are also highly clustered as characterized by the clustering coefficient. The latter is defined by  $C_i = 2y_i/k_i(k_i - 1)$  where  $k_i$  is the degree of node  $i$  and  $y_i$  is the number of links between its neighbors. The large ratios  $C = \bar{C}/C_{ER}$  of the average values with respect to those of Erdős-Rényi (ER) random graphs of the same sizes confirm the high clustering that is present in these networks.

A very fruitful concept that has led to a unifying view on complex networks and also leads to their classification is that of scale-free behavior [1]. If  $p(k)$ , the probability that given node of the network has degree  $k$ , follows a power law  $p(k) \sim k^{-\gamma}$ , indicating a fat tail of the node degree distribution, the network is said to be scale-free. While many networks and in particular random graphs

have an exponentially or even faster decaying distribution  $p(k)$ , it has been shown that an evolutionary growth procedure with preferential attachment to high degree nodes leads to scale-free behavior [14]. Furthermore, for many applications scale-free and small world networks emerge naturally upon optimization for minimizing both the costs for communication and maintenance [15] which are central criteria for the design of PTNs.

Using scaling arguments for tree graphs the dependence of a number of properties of scale-free networks on the exponent  $\gamma$  has been worked out. In particular, the value of  $\gamma$  discriminates between different classes for the percolation behavior: if  $\gamma > 4$ , the behavior is equivalent to that of networks with exponential  $p(k)$ , while it is qualitatively different for  $\gamma < 4$ , moreover there is no percolation threshold for  $2 < \gamma \leq 3$  [16]. The percolation threshold is given by:  $\kappa \equiv \overline{k^2}/\overline{k} = 2$ . For the PTNs studied this ratio is listed in Table I. Finding a network with  $\kappa$  near the threshold means that it is vulnerable against failure in the sense that inactivating a small number of nodes may break the network into disconnected clusters. The Table shows that all PTNs are clearly above this threshold, for some of them  $\kappa$  indicates an especially strong resilience against failure [11].

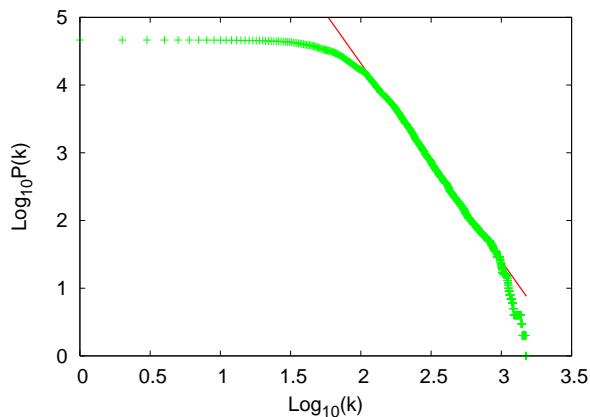


FIG. 2: Integrated node degree distribution  $P(k) = \int_k^{k_{\max}} p(k)dk$  for the Los Angeles PTN in  $\mathbf{P}$ -space with fit to a power law.

More information can be gained by fitting the degree distribution to a power-law as above or to an exponential function  $p(k) \sim \exp(-k/\hat{k})$  observing the quality of the fit. In Table I we list the results of both fits for the  $\mathbf{L}$  and  $\mathbf{P}$ -spaces. In the  $\mathbf{L}$ -space representation, the  $p(k)$  of eight cities is found to be well fitted by a power law with  $\gamma$  values between 2.6 and 5. The corresponding results for the exponential fits for these cities are given in parentheses. The other six cities are rather governed by an exponentially decaying  $p(k)$  (for these, the power law fit is shown in parentheses). Whereas the scale-free behavior in the  $\mathbf{L}$ -space has also been seen in previous work [9, 10], such behavior was ruled out for the  $\mathbf{P}$ -space

[9]. Fig. 2 however clearly indicates that the  $\mathbf{P}$ -space node degree distribution of the Los Angeles PTN follows a power-law with exponent  $\gamma_p = 3.9$ . The same also applies to London and Paris, all other cities appear to have an exponentially decaying  $p(k)$  in this space. Whereas an exponential distribution may be explained by a random placement of the routes, the power law found for the three cities indicates that the routes are organized in a correlated way. The deeper reasons for this special behavior currently remain unclear.

Using the full information about the route paths as included in the  $\mathbf{L}'$ -representation with colored links (Fig. 1), we can extract specific PTN features. One of them is that several routes may proceed in parallel on a common road or track for a sequence of stations. The emerging picture very much resembles networks found in car wiring technology, where the term *harness* is used. To quantitatively describe this characteristic we introduce the harness distribution  $P(r, s)$ : the number of sequences of  $s$  consecutive stations that are serviced by  $r$  parallel routes. In Fig. 3a we show the harness distribution for the PTN of Sydney. The log-log plot indicates that also this distribution appears to be scale-free. Similar behavior was found for most of the cities included in our study.

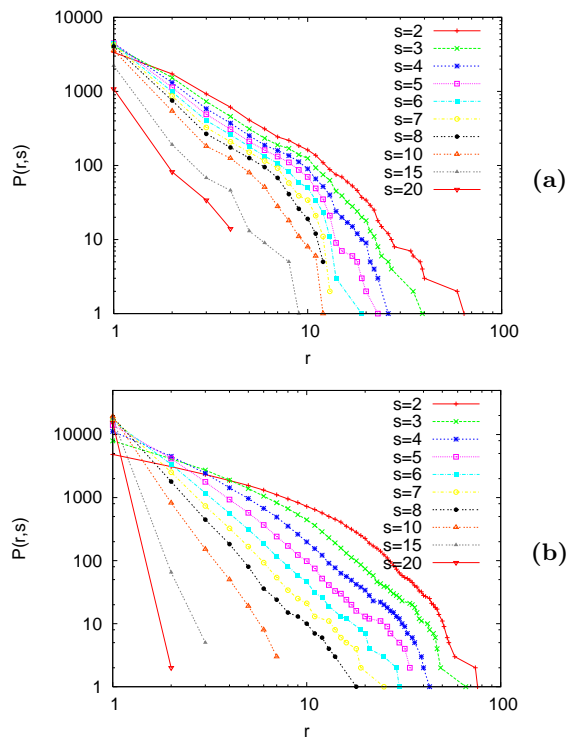


FIG. 3: Harness distribution: number of sequences of  $s$  consecutive stations that are serviced by  $r$  parallel routes. a: Sydney PTN, b: simulated city with  $a = 0, b = 0.5$ .

The evidence for the scale-free properties of PTNs presented so far encourages us to propose an evolutionary

growth model for these networks along the following lines: We model the grid of streets by a quadratic 2D lattice and allow every lattice site  $\vec{r}$  (street corner) to be a potential station visited by e.g.  $k_{\vec{r}}$  routes. The routes are modeled as self-avoiding walks (SAWs) on this lattice. This model captures the typical meandering of the routes to optimize the coverage of neighborhoods. Obviously, real routes are also planned to access sites of interest. These serve as points of attraction of the walks and ‘integrating out’ their specific locations one is left with an effective attraction between the routes.

The rules of our model are the following:

1. First route: construct a SAW of length  $n$ .
2. Subsequent routes: (i) choose a terminal station at the lattice site  $\vec{r}$  with probability  $q \sim k_{\vec{r}} + a$ ; (ii) choose a subsequent station of this route at a neighboring site  $\vec{r}'$  with probability  $q \sim k_{\vec{r}'} + b$ ; (iii) repeat step (ii) until the walk has reached  $n$  stations, in case of self-intersection discard the walk and restart with step (i).
3. Repeat step 2 until  $m$  routes are created.

Implementing the model on a 2D lattice implies the assumption of a PTN growing in a regular isotropic uncorrelated environment. While it is natural that the routes should not intersect themselves, the hypothesis that apart from the effective attraction they otherwise proceed randomly may not be obvious. SAWs are well studied in physics to model scaling properties of polymers and polymer networks [17]. In 2D, the end-to-end distance  $R$  of a SAW of  $N$  steps is known to scale for large  $N$  as  $R \sim N^\nu$  with an exact result for the exponent  $\nu = 3/4$  [18]. This result as well as other scaling properties remain unperturbed even on a weakly disordered lattice as long as the disorder is not long-range correlated [19]. This supports our choice of disregarding such possible disturbances of the lattice in our model. We have tested this hypothesis using publicly available geographical data [20] for the stations of the Berlin PTN. Plotting the root mean square distance  $R$  as function of the number of stations traveled starting from a terminal we find surprising agreement with the 2D SAW behavior (see Fig. 4). Furthermore, the corresponding result for a simulated city confirms this picture. Apparently, the SAW balances between area coverage and traveling time.

In Table I we have included the characteristics as extracted from simulated PTNs with  $m = 500$  routes each of  $n = 50$  stations for typical parameters  $a$  and  $b$ . In particular our model is nicely suited to reproduce the harnessing effect of the PTNs as shown in Fig. 3b. Varying the parameter  $b$  for  $a = 0$  we observe a crossover from scale-free behavior in  $\mathbf{P}$ -space for small  $b$  to an exponential one as  $b$  increases beyond 1. Some  $\mathbf{L}$ -space characteristics we left blank in the table due to artifacts of the

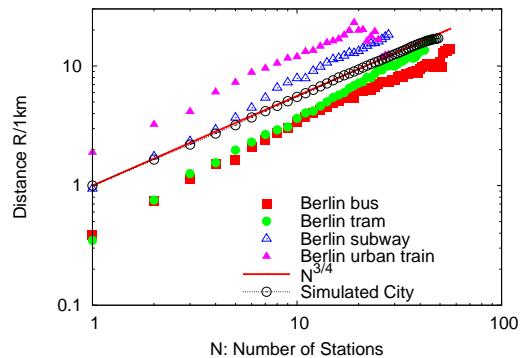


FIG. 4: Berlin PTN:  $R$  as function of the number of stations traveled compared with the 2D SAW and a simulated city with parameters  $a = 0, b = 0.5$ .

square lattice neighborhood. Although our growth rules look very similar to usual network evolution by preferential attachment [14], there is no simple relation between the parameters  $a$  and  $b$  and the exponent  $\gamma$  even in the scale-free scenario. The principal difference of our algorithm is that at each step we link an *existing* station to a neighboring site which does not need to be empty. New stations are then only added at the frontier of the PTN cluster while high degree nodes (hubs) accumulate at its center.

Our analysis of PTNs of so far unexplored sizes brings about that very large PTNs may display scale free  $\mathbf{P}$ -space distributions and confirms corresponding  $\mathbf{L}$ -space results [9, 10]. The surprising SAW behavior of the routes encouraged us to analyze an evolutionary model of mutually attractive SAWs which reproduces a number of key features of PTNs. In conclusion, we want to emphasize the importance of the constraints that are imposed on the network by the area consuming links when it is embedded in a 2D space. The harnessing effect presented in this study being a first example. Similar problems are met e.g. for electric circuit design.

We acknowledge support by the EC under the Marie Curie Host Fellowships for the Transfer of Knowledge, project COCOS, contract MTKD-CT-2004-517186 (C.v.F.), and Austrian Fonds zur Förderung der wissenschaftlichen Forschung under Project P16574 (Yu.H.).

\* ferber@physik.uni-freiburg.de

- [1] R. Albert and A.-L. Barabási, Rev. Mod. Phys. **74**, 47 (2002); S.N. Dorogovtsev and J.F.F. Mendes, Adv. Phys. **51**, 1079 (2002); M.E.J. Newman, SIAM Review **45**, 167 (2003); S.N. Dorogovtsev and J.F.F. Mendes, *Evolution of Networks* (Oxford University Press, Oxford, 2003).
- [2] L.A.N. Amaral, A. Scala, M. Barthélémy, and H.E. Stanley, Proc. Nat. Acad. Sci. USA., **97**, 11149 (2000).
- [3] R. Guimerà and L.A.N. Amaral, Eur. Phys. J. B **38**, 381

- (2004); R. Guimera, S. Mossa, A. Turtleschi, and L.A.N. Amaral, Proc. Nat. Acad. Sci. USA **102**, 7794 (2005); A. Barrat, M. Barthélemy, R. Pastor-Satorras, and A. Vespignani, Proc. Nat. Acad. Sci. USA **101**, 3747 (2004); W. Li and X. Cai, Phys. Rev. E **69**, 046106 (2004); W. Li, Q.A. Wang, L. Nivanen, and A. Le Méhauté, e-print physics/0601091.
- [4] P. Sen, S. Dasgupta, A. Chatterjee, P.A. Sreeram, G. Mukherjee, and S.S. Manna, Phys. Rev. E **67**, 036106 (2003)
- [5] P. Crucitti, V. Latora, and M. Marchiori, Physica A **338**, 92 (2004); R. Albert, I. Albert, and G.L. Nakarado, Phys. Rev. E **69**, 025103(R) (2004).
- [6] M. Marchiori and V. Latora, Physica A **285**, 539 (2000).
- [7] V. Latora and M. Marchiori, Phys. Rev. Lett. **87**, 198701 (2001); V. Latora and M. Marchiori, Physica A **314**, 109 (2002).
- [8] K.A. Seaton and L.M. Hackett, Physica A **339**, 635 (2004).
- [9] J. Sienkiewicz and J.A. Holyst, Phys. Rev. E **72**, 046127 (2005).
- [10] C. von Ferber, Yu. Holovatch, and V. Palchykov, Condens. Matter Phys. **8**, 225 (2005).
- [11] C. von Ferber, T. Holovatch, Yu. Holovatch, and V. Palchykov, in preparation.
- [12] For links see: <http://www.apta.com>.
- [13] D.J. Watts, S.H. Strogatz, Nature **393**, 440 (1998).
- [14] A.-L. Barabási and R. Albert, Science **286**, 509 (1999); A.-L. Barabási, R. Albert, and H. Jeong, Physica A **272**, 173 (1999).
- [15] S. Valverde, R. Ferrer Cancho, and R.V. Solé, Europhys. Lett. **60**, 512 (2002); M.T. Gastner and M.E.J. Newman, Eur. Phys. J. B **49**, 247 (2006); N. Mathias and V. Gopal, Phys. Rev. E **63**, 021117 (2001).
- [16] R. Cohen, D. ben-Avraham, and S. Havlin, Phys. Rev. E **66**, 036113 (2002).
- [17] P.-G. de Gennes, *Scaling Concepts in Polymer Physics* (Cornell University Press, Ithaca and London, 1979).
- [18] B. Nienhuis, Phys. Rev. Lett. **49**, 1062 (1982).
- [19] A.B. Harris, Z. Phys. B **49**, 347 (1983); V. Blavats'ka, C. von Ferber, and Yu. Holovatch, Phys. Rev. E, **64**, 041102 (2001); C. von Ferber and Yu. Holovatch, Phys. Rev. E **65**, 042801 (2002); C. von Ferber, V. Blavats'ka, R. Folk, and Yu. Holovatch, Phys. Rev. E **70**, 035104(R) (2004).
- [20] For maps see: <http://www.fahrinfo-berlin.de>.